Global Energy Interconnection
Development and Cooperation Organization

Volume 4 Number 2 April 2021 (126-135)
DOI: 10.14171/j.2096-5117.gei.2021.02.002

Global Energy Interconnection

Contents lists available at ScienceDirect
https: //www.sciencedirect.com/journal/global-energy-interconnection

Full-length article

Distributed generator-based distribution system service restoration strategy and model-free control methods

Weijia Liu, Yue Chen, Fei Ding

Power System Engineering Center, National Renewable Energy Laboratory, 15013 Denver West Pkwy, Golden, CO 80401, USA

Scan for more details

Abstract: The rapid growth of distributed generator (DG) capacities has introduced additional controllable assets to improve the performance of distribution systems in terms of service restoration. Renewable DGs are of particular interest to utility companies, but the stochastic nature of intermittent renewable DGs could have a negative impact on the electric grid if they are not properly handled. In this study, we investigate distribution system service restoration using DGs as the primary power source, and we develop an effective approach to handle the uncertainty of renewable DGs under extreme conditions. The distribution system service restoration problem can be described as a mixed-integer second-order cone programming model by modifying the radial topology constraints and power flow equations. The uncertainty of renewable DGs will be modeled using a chance-constrained approach. Furthermore, the forecast errors and noises in real-time operation are solved using a novel model-free control algorithm that can automatically track the trajectory of real-time DG output. The proposed service restoration strategy and model-free control algorithm are validated using an IEEE 123-bus test system.

Keywords: Distribution system service restoration, Distributed generator (DG), Intermittent renewable energy sources, Model-free control, Power system resilience, Uncertainty management

0 Introduction

Distribution system service restoration represents the power supply recovery process for electricity consumers in distribution systems after faults or power failures. Recent years have witnessed an increasing number of power outages associated with extreme weather events, such as the 2008 blackout in China caused by an extremely heavy snowstorm and the 2012 blackout in the United States caused by Hurricane Sandy [1]–[2]. Compared to transmission systems that usually have a meshed topology and redundant generation capacity, distribution systems typically have a limited number of sectionalizing switches and generation resources. Therefore, bulk transmission grids are more resilient to extreme events than distribution systems, meaning that the increasing threats of extreme events are more likely to devastate the power supply in distribution systems and lead to enormous social and economic losses [3]–[4].

Traditionally, distribution systems have relied exclusively on the power supply from bulk power systems, and they do not have the capability to restore load supply services when upstream transmission systems

Received: January 20 2021 Accepted: March 5 2021 Published: April 25 2021

Weijia Liu
weijia.liu@nrel.gov

Fei Ding
fei.ding@nrel.gov

Yue Chen
yue.chen@nrel.gov

are experiencing major disturbances. This situation has changed because of the integration of distributed generators (DGs) in modern distribution systems. Distribution systems can leverage the capacity and flexibility of DGs to provide emergency power to critical interrupted loads when suffering from a major power outage and thus improve system resilience. The uncertainty associated with renewable DGs (e.g., wind turbines and solar panels), however, brings another challenge to DG-based distribution system service restoration; hence, the development of an effective distribution system service restoration strategy that can properly handle the uncertainty of DGs is of significant importance to distribution utilities.

Existing research has explored the key issues during restoration in cases of distribution system failures, such as the general principles of distribution network restoration through reconfiguration [5], optimization of switch and tap-changer reconfiguration [6], fuzzy decision-making restoration model [7], service restoration strategy considering multiple faults [8], and reconfiguration strategy for large radial distribution networks [9]. Distribution system outages caused by transmission system failures, however, are more difficult to recover because of the lack of reliable power sources. The application of DGs in distribution system service restoration has been addressed in existing work, such as service restoration with distributed energy storage [10], DG-based restoration considering cold-load pickup characteristics [11], microgrids as black-start sources [12]–[14], and the distribution restoration strategy based on microgrids and the spanning tree search methodology [15].

These studies validated the feasibility of implementing DGs for distribution system service restoration; however, the DG generation capacity in these studies is generally redundant so that a reasonable restoration strategy can successfully leverage the flexibility of DGs to recover the interrupted load supply. Unfortunately, the installed DG capacity in most existing utility distribution systems is quite limited, and renewable DGs are stochastic [16]. If the DG devices are not capable of supplying all interrupted loads in the distribution systems, a proportion of outage loads will not be supplied and will remain isolated to guarantee the reliability of recovered systems/microgrids. In fact, little attention has been paid to restoration problems with insufficient distributed generation capabilities. To better use the generation capabilities of distributed energy resources (DERs) and supply sustainable power to as many loads as possible after a blackout, this study focuses on the distribution system restoration problem with a limited capacity of intermittent renewable DGs.

Another important issue that has not been properly addressed in existing literature is the real-time DG control methods during service restoration. On one hand, the forecast error of renewable DGs is inevitable. On the other hand, the renewable DG outputs are volatile and can change rapidly over time. Because they are the primary power sources during service restoration, a reasonable control method is needed to ensure that renewable DGs can act as reliable and sustainable power supplies. Existing DG control methods generally require an accurate system model to achieve the optimal control objective [17]–[18], whereas distribution system models and parameters can become unreliable when suffering from major disturbances such as power outages. Therefore, it is critical to investigate a real-time control method that can effectively track the trajectory of renewable DG outputs and does not rely on system model knowledge.

In this study, we propose a mixed-integer second-order cone programming (SOCP) model to optimize the distribution system service restoration by leveraging the DG contributions. The forecast error of renewable DGs will be handled by a chance-constrained approach and will be integrated into the proposed model to be efficiently solved by commercial solvers. When executing the optimized service restoration solutions, a model-free real-time control method is developed to track the renewable DG outputs and maintain the stability and reliability of restored systems without knowledge of the accurate system model. In this manner, distribution system operators can effectively perform service restoration based on local DGs to improve the distribution system resilience.

The remainder of this paper is organized as follows. Section 1 introduces the service restoration model with DG devices. Section 2 describes the employed model-free control method for real-time DG control. Section 3 presents the simulation results. Section 4 concludes the paper.

1 Service restoration planning model

Generally, DGs can have diverse characteristics in terms of fuel type, capacity, and ownership. Small capacity DGs (e.g., a few kWs) are mostly owned and operated by private customers; thus, these small DGs can be difficult to control and coordinate. Utility-scale DGs typically have much larger capacities (e.g., hundreds of kWs) and are owned or operated by utility companies. When suffering from power outages, utility-scale DGs can effectively follow control signals and provide considerable generation capacities; therefore, it is assumed that utility-scale DGs will be the primary power sources during service restoration. When an outage occurs, the utility system operator coordinates the operation of utility-scale DGs to recover the power supply to outage loads.

1.1 Service restoration model

If the available generation capacities of DERs are not sufficient or reliable to supply all the outage loads in the distribution system, one or several restoration islands will be formed, and the DERs will be responsible for supplying power to the loads within their supply region. Basically, the restoration of a distribution system aims to maximize the capacity of restored loads and is subject to the characteristics of DERs and distribution system constraints, that is,

$$\text{Max} \sum_{i\in\Omega_T}\sum_{i\in\Omega_N}\varphi_i P_{i,t}^{D} \tag{1}$$

$$\text{s.t.} \quad P_{i,t}^{G\min} \leqslant (1+\varpi)P_{i,t}^{G} \leqslant P_{i,t}^{G\max} \tag{2}$$

$$Q_{i,t}^{G\min} \leqslant (1+\varpi)Q_{i,t}^{G} \leqslant Q_{i,t}^{G\max} \tag{3}$$

$$V_i^{\min} \leqslant V_{i,t} \leqslant V_i^{\max} \tag{4}$$

$$-z_{ij}I_{ij}^{\max} \leqslant I_{ij,t} \leqslant z_{ij}I_{ij}^{\max} \tag{5}$$

$$P_{i,t}^{G} - P_{i,t}^{D} = V_{i,t}\sum_{j\in\Omega_N}V_{j,t}(g_{ij}\cos\theta_{ij,t}+b_{ij}\sin\theta_{ij,t}) \tag{6}$$

$$Q_{i,t}^{G} - Q_{i,t}^{D} = V_{i,t}\sum_{j\in\Omega_N}V_{j,t}(g_{ij}\sin\theta_{ij,t}-b_{ij}\cos\theta_{ij,t}) \tag{7}$$

$$z_{ij} \in \{0,1\}, \forall ij \in \Omega_L \tag{8}$$

where z_{ij} is the Boolean variable for distribution lines, a positive value means that line ij is restored, and vice versa; Ω_N, Ω_L, and Ω_T denote the sets of distribution system nodes, distribution lines, and considered restoration time intervals, respectively; φ_i denotes the weighting factor of the interrupted load at bus i. The weighting factor is intended to distinguish the load priorities and can be determined based on the economic loss associated with per-unit energy consumption; $P_{i,t}^{D}$, $Q_{i,t}^{D}$, $P_{i,t}^{G}$, and $Q_{i,t}^{G}$ are the active/reactive load capacity and active/reactive power generation of the DER at node i, respectively; $P_{i,t}^{G\max}$, $P_{i,t}^{G\min}$, $Q_{i,t}^{G\max}$, and $Q_{i,t}^{G\min}$ are the maximum/minimum available active and reactive power DER outputs at node i, respectively; ϖ represents the required reserve coefficient; $V_{i,t}$, $V_i^{\max}$, and $V_i^{\min}$ are the nodal voltage magnitude and its maximum and minimum values at node i, respectively; $I_{ij,t}$ and $I_{ij}^{\max}$ denote the current magnitude and its maximum limit of line ij; $\theta_{ij,t}$, g_{ij}, and b_{ij} denote the phase angle between node i and node j, and the real part and the imaginary part of the (i, j)-th entry of the nodal admittance matrix, respectively. The radiality of the restored distribution islands should be guaranteed by introducing graph theory-based constraints, which will be discussed in Section 1.2.

This distribution system restoration model contains integer variables and nonlinear constraints, which makes it difficult to solve directly. In this study, the network radiality and AC power flow constraints are modified to reduce the restoration model complexity.

1.2 Network radiality constraints

Spanning tree constraints are widely used in existing literature to guarantee the radial topology of distribution systems. The original constraints should be revised to accommodate cases where multiple islands should exist; therefore, for distribution system service restoration problems with DGs, the spanning tree constraints can be revised as follows:

$$\mu_{ij}^{1} + \mu_{ij}^{2} = z_{ij}, ij \in \Omega_L \tag{9}$$

$$\mu_{ij}^{1} \geqslant 0, \mu_{ij}^{2} \geqslant 0, ij \in \Omega_L \tag{10}$$

$$\sum_i \mu_{ij}^{1} = 1, \forall j \in \Omega_N, j \notin \Omega_S \tag{11}$$

$$\sum_i \mu_{ij}^{1} = \tau_j, \forall j \in \Omega_S \tag{12}$$

$$\sum_{j\in\Omega_S} \tau_j = N_S - N_B + z^T z \tag{13}$$

$$\tau_j \in \{0,1\}, \forall j \in \Omega_S \tag{14}$$

where μ_{ij}^{1} and μ_{ij}^{2} are auxiliary continuous variables that indicate the direction of the power flow of line ij. Ω_S denotes the set of DG buses, and N_S and N_B denote the number of DGs and buses, respectively. τ_j is a Boolean variable that determines the injected flow direction of DG node j.

Constraints (9) – (14) can manage situations where the number of restored islands is not determined. If multiple DGs are to be assigned to one island, only one of them will be considered as the source, according to (12) – (14); thus, (9) – (14) guarantee that all the restored islands are radial. Note that loops may be acceptable in distribution feeders under certain circumstances. In such cases, (9) – (14) can be neglected to formulate more flexible islanding strategies.

Remark: To maintain a steady restoration topology and avoid frequent switch operations, the Boolean variable z_{ij} is not time-variant, indicating that the topology will remain unchanged for the entire restoration duration ($\forall t \in \Omega_T$). Hence, the number of restoration time intervals (i.e., the cardinality of the set Ω_T) has a significant impact on the finalized restoration solutions. To minimize the influence of renewable DG forecast errors and maintain the flexibility of topological changes, utility companies should determine the restoration time interval based on: 1) the renewable DG generation forecast accuracy over time and 2) the acceptable switch operation interval. In this study, each time interval was set to 15 min and the total restoration horizon was

3 h because the short-term renewable DG forecast was relatively accurate.

1.3 Model convexification

The AC power flow equations in radial distribution networks can be converted into various forms by different methods to eliminate the nonlinearities introduced by the sine and cosine functions [19]–[20]. Although the AC power flows cannot be converted into linear constraints without approximation, they can be transferred into SOCP equations, which can be efficiently solved by commercial solvers. By employing the methods described in [20] and ignoring the shunt susceptance of the distribution lines, the nonlinear constraints in (4) – (7) are transformed as follows:

$$P_{i,t}^{\mathrm{G}} - P_{i,t}^{\mathrm{D}} = \sum_{j \in \Omega_{\mathrm{N}}} \left(g_{ij} U_{i,t} - g_{ij} W_{ij,t} - b_{ij} C_{ij,t} \right) \tag{15}$$

$$Q_{i,t}^{\mathrm{G}} - Q_{i,t}^{\mathrm{D}} = \sum_{j \in \Omega_{\mathrm{N}}} \left(-b_{ij} U_{i,t} + b_{ij} W_{ij,t} - g_{ij} C_{ij,t} \right) \tag{16}$$

$$U_{i,t} = \left(V_{i,t} \right)^2 \tag{17}$$

$$W_{ij,t} = W_{ji,t} \tag{18}$$

$$C_{ij,t} = -C_{ji,t} \tag{19}$$

$$U_{i,t} U_{j,t} - \left(W_{ij,t} \right)^2 - \left(C_{ij,t} \right)^2 \geqslant 0 \tag{20}$$

$$\left(V_i^{\min} \right)^2 < U_{i,t} < \left(V_i^{\max} \right)^2 \tag{21}$$

$$\left(I_{ij,t} \right)^2 \leqslant z_{ij} \left(I_{ij}^{\max} \right)^2 \tag{22}$$

$$\left(I_{ij,t} \right)^2 = \left(g_{ij}^2 + b_{ij}^2 \right) \left(U_{i,t} + U_{j,t} - 2W_{ij,t} \right) \tag{23}$$

where $U_{i,t}$, $W_{ij,t}$, and $C_{ij,t}$ are introduced as auxiliary variables. Equations (15) – (23) are sufficient to convert the AC power flow equations of radial distribution systems into SOCP problems. Combined with the network radiality constraints (9) – (14), the optimization model is a mixed-integer SOCP problem.

Note that the inequality constraint (20) is a relaxation to maintain model convexity. Typically, SOCP relaxation is exact for radial distribution systems. Thus, relaxing (20) will not affect the accuracy because constraints (9) – (14) ensures the radiality of reconfigured networks. More discussions concerning the exactness of SOCP relaxation can be found in studies such as [21].

1.4 Uncertainty modeling

The uncertainty of renewable DGs will directly influence the nodal active power injection and further affect the optimality and sometimes the feasibility of distribution system restoration strategies. In this section, a chance-constrained approach is employed to model the uncertainty factors when optimizing the restoration planning model.

Let $P_{i,t}^{\mathrm{Gmax,u}}$ and $P_{i,t}^{\mathrm{Gmax,l}}$ denote the upper and lower forecasted limits of $P_{i,t}^{\mathrm{Gmax}}$ at a confidence level of α_i at time t, respectively. Thus, the chance constraint can be adopted to reformulate (2) as:

$$P_{i,t}^{\mathrm{Gmin}} \leqslant (1+\varpi) P_{i,t}^{\mathrm{G}} \leqslant P_{i,t}^{\mathrm{Gmax}} \tag{24}$$

$$P_r \left\{ P_{i,t}^{\mathrm{Gmax,l}} \leqslant P_{i,t}^{\mathrm{Gmax}} \leqslant P_{i,t}^{\mathrm{Gmax,u}} \right\} \geqslant \alpha_i \tag{25}$$

where P_r is the probability measure.

In general, $Q_{i,t}^{\mathrm{Gmax}}$ and $Q_{i,t}^{\mathrm{Gmin}}$ of renewable DGs are constrained by the rated capacity of their inverters [22]. In this study, they are conservatively calculated as,

$$Q_{i,t}^{\mathrm{Gmax}} = -Q_{i,t}^{\mathrm{Gmin}} = \sqrt{\left(S_i^{\mathrm{G}} \right)^2 - \left(P_{i,t}^{\mathrm{Gmax,u}} \right)^2} \tag{26}$$

where S_i^{G} represents the inverter capacity of the i-th DG.

Equation (25) is normally handled by methods such as Monte Carlo simulation [23], which is generally considered computationally inefficient. Employing $P_{i,t}^{\mathrm{Gmax,l}}$ as the estimated $P_{i,t}^{\mathrm{Gmax}}$ could be a fast and feasible solution, but the results might be too conservative because it is less likely that the actual power output of each DER is near its estimated lower limit at the same time.

The probabilistic distribution function of renewable DG generation output is typically difficult to derive. However, the forecast error between the generation forecast and actual output can be modeled by the normal distribution as described below:

$$P_{i,t}^{\mathrm{Gmax}\oplus} - \mu_{i,t}^{\mathrm{G}} \sim N(0, (\sigma_{i,t}^{\mathrm{G}})^2) \tag{27}$$

$$\mu_{i,t}^{\mathrm{G}} = \frac{1}{2} (P_{i,t}^{\mathrm{Gmax,l}} + P_{i,t}^{\mathrm{Gmax,u}}) \tag{28}$$

$$\sigma_{i,t}^{\mathrm{G}} = \frac{(P_{i,t}^{\mathrm{Gmax,u}} - P_{i,t}^{\mathrm{Gmax,l}})}{2\Phi^{-1}\left(\dfrac{1+\alpha_i}{2} \right)} \tag{29}$$

where $P_{i,t}^{\mathrm{Gmax}\oplus}$ denotes the actual available power output of the DG at node i at time t; $\mu_{i,t}^{\mathrm{G}}$ and $\sigma_{i,t}^{\mathrm{G}}$ denote the expectation of the forecast $P_{i,t}^{\mathrm{Gmax}}$ and the standard deviation of forecast error between $P_{i,t}^{\mathrm{Gmax}\oplus}$ and $\mu_{i,t}^{\mathrm{G}}$, respectively; and Φ^{-1} denotes the inverse function of the cumulative distribution function of the standard normal distribution.

Assume that there exist Ψ intermittent DGs, and the correlation coefficient between any two DGs is known a priori. The covariance matrix of the DG forecast error, denoted as $\boldsymbol{\Theta}$, can be calculated as,

$$\boldsymbol{\Theta} = \left[\vartheta_{i,j} \right]_{\Psi \times \Psi} \quad i, j = 1, 2, ..., \Psi \tag{30}$$

$$\vartheta_{i,j} = \begin{cases} (\sigma_{i,t}^{\mathrm{G}})^2 & i=j \\ \rho_{ij} \sigma_{i,t}^{\mathrm{G}} \sigma_{j,t}^{\mathrm{G}} & i \neq j \end{cases} \tag{31}$$

where $\vartheta_{i,j}$, and ρ_{ij} denote the covariance and correlation coefficient between DG i and j, respectively.

Integrating $\boldsymbol{\Theta}$ into evaluating DG output uncertainties alleviates the conservative estimation, and the generation capabilities of the DERs can be better used. As a result, (27) can be modified as,

$$P_{i,t}^{\mathrm{Gmax}} \leqslant \mu_{i,t}^{\mathrm{G}} + \Phi^{-1}\left(\frac{1+\alpha_i}{2}\right)\sqrt{\boldsymbol{\pi}_{(i,:)}\boldsymbol{\Theta}\boldsymbol{\pi}_{(i,:)}^{\mathrm{T}}} \tag{32}$$

$$P_{i,t}^{\mathrm{Gmax}} \geqslant \mu_{i,t}^{\mathrm{G}} - \Phi^{-1}\left(\frac{1+\alpha_i}{2}\right)\sqrt{\boldsymbol{\pi}_{(i,:)}\boldsymbol{\Theta}\boldsymbol{\pi}_{(i,:)}^{\mathrm{T}}} \tag{33}$$

where $\boldsymbol{\pi}_{(i,:)}$ denotes the i-th entry of the DG active power generation sensitivity vector, which can be calculated based on [24]–[25]. Note that (32) and (33) are linear approximations of (25). Nonetheless, they are more computationally efficient than (25) and less conservative than using $P_{i,t}^{\mathrm{Gmax,l}}$ as the available power generation of renewable DGs.

1.5 Complete model formulation

Let $S_{i,t} = \left[P_{i,t}^{\mathrm{G}}, P_{i,t}^{\mathrm{D}}, Q_{i,t}^{\mathrm{G}}, Q_{i,t}^{\mathrm{D}}, P_{i,t}^{\mathrm{Gmax}}\right]^{\mathrm{T}}$. The complete mathematical model for distribution system restoration can be described as follows:

$$\max_{S_{i,t},\mu_{ij}^1,\mu_{ij}^2,z_{ij},\tau_j,U_{i,t},W_{ij,t},C_{ij,t}} \sum_{t\in\Omega_{\mathrm{T}}}\sum_{i\in\Omega_{\mathrm{N}}} \varphi_i P_{i,t}^{\mathrm{D}}$$
$$s.t. (2),(3),(8)-(23),(32),(33)$$

2 Model-free control algorithm

Section 1.4 employed a chance-constrained approach to model the uncertainty of renewable DGs, but the forecast error and renewable DG output fluctuations are still inevitable. When the generation of renewable DGs is redundant, the distribution system can supply more interrupted loads to minimize economic loss. If the generation of renewable DGs falls below expectations, additional generation resources should kick in to maintain the reliability of the restored system. Therefore, the real-time control algorithm should be able to track the trajectory of renewable DG generation and adjust the operational strategy in a timely fashion.

Another concern lies in the accuracy of the distribution system models. Typically, utility companies do not have accurate data on secondary feeders. Further, extreme events such as natural disasters can cause various faults/malfunction scenarios that are difficult to model and detect; thus, traditional model-based control algorithms might become infeasible when dealing with distribution system restoration problems. A model-free real-time control algorithm that can achieve satisfactory control performance without relying on accurate system models is desired.

The employed real-time model-free control algorithm is demonstrated using a general optimization problem described in (34)–(36) as an example. For DG-based distribution system service restoration, the real-time control objective is to use renewable DG outputs and reduce load curtailment:

$$\text{Min } f_0^{(k)}\left(\boldsymbol{y}^{(k)}(\boldsymbol{x})\right) + \sum_{m=1}^{M} f_m^{(k)}(\boldsymbol{x}_m) \tag{34}$$

$$\text{s.t. } \boldsymbol{x}_m \in \boldsymbol{\chi}_m^{(k)}, m = 1,2,\ldots,M \tag{35}$$

$$g_n^{(k)}\left(\boldsymbol{y}^{(k)}(\boldsymbol{x})\right) \leqslant 0, n = 1,2,\ldots,N \tag{36}$$

where $\boldsymbol{\chi}_m^{(k)}$ is a convex set representing the feasibility region of control input $\boldsymbol{x}_m$ of system m at control step k, and $\boldsymbol{y}^{(k)}(\boldsymbol{x})$ is an algebraic formulation of observable system outputs. $f_0^{(k)}()$ is a time-varying function associated with $\boldsymbol{y}^{(k)}(\boldsymbol{x})$. $g_n^{(k)}()$ denotes the time-varying constraints on $\boldsymbol{y}^{(k)}(\boldsymbol{x})$.

Naturally, this method is model-based, and the Lagrangian-based control method can be described as,

$$\boldsymbol{x}^{(k+1)} = \mathrm{Proj}_{\chi^{(k)}}\left\{(1-\alpha)\boldsymbol{x}^{(k)} - \alpha\begin{pmatrix}\nabla_x f^{(k)}\left(\boldsymbol{x}^{(k)}\right) + \\ \boldsymbol{C}^T\nabla_y f_0^{(k)}\left(\hat{\boldsymbol{y}}^{(k)}\right) + \sum_{m=1}^{M}\lambda_m^{(k)}\boldsymbol{C}^T\nabla g_m^{(k)}\left(\hat{\boldsymbol{y}}^{(k)}\right)\end{pmatrix}\right\} \tag{37}$$

$$\lambda_m^{(k+1)} = \mathrm{Proj}\left\{(1-\alpha)\lambda_m^{(k)} + \alpha\boldsymbol{g}^{(k)}\left(\hat{\boldsymbol{y}}^{(k)}\right)\right\} \tag{38}$$

where $\alpha > 0$ is a constant step size, and $\hat{\boldsymbol{y}}^{(k)}$ is the measurement of $\boldsymbol{y}^{(k)}(\boldsymbol{x}^{(k)})$. Note that the control algorithm (37)–(38) still relies on the knowledge of the system model $\boldsymbol{C}^{\mathrm{T}}$.

To derive a model-free variant of (37) and (38), we first look at Taylor's theorem. For any $r \in \mathbb{R}$, we have,

$$F(\boldsymbol{x}+r\boldsymbol{\xi}) = F(\boldsymbol{x}) + r\boldsymbol{\xi}^T\nabla F(\boldsymbol{x}) + \frac{r^2}{2}\boldsymbol{\xi}^T\nabla^2 F(\boldsymbol{x})\boldsymbol{\xi} + O\left(r^3\right) \tag{39}$$

Taking $r = \in$ and $r = -\in$, the contraction yields:

$$F(\boldsymbol{x}+\in\boldsymbol{\xi}) - F(\boldsymbol{x}-\in\boldsymbol{\xi}) = 2\in\boldsymbol{\xi}^{\mathrm{T}}\nabla F(\boldsymbol{x}) + O\left(\in^3\right) \tag{40}$$

where $\in\boldsymbol{\xi}$ indicates that the variable $\boldsymbol{x}$ is perturbed by $\pm\in\boldsymbol{\xi}$.

Therefore, the gradient can be approximated by:

$$\hat{\nabla}F(\boldsymbol{x}) = \frac{1}{2\in}\boldsymbol{\xi}\left[F(\boldsymbol{x}+\in\boldsymbol{\xi}) - F(\boldsymbol{x}-\in\boldsymbol{\xi})\right] \tag{41}$$

As shown in (41), the gradient approximation no longer requires knowledge of the system model $\boldsymbol{C}^{\mathrm{T}}$. Returning to the discussed general optimization problem (34)–(36), the approximated Lagrangian can be calculated as,

$$\hat{\nabla}\mathrm{L}^{(k)} = \nabla_x f^{(k)}\left(\boldsymbol{x}^{(k)}\right) + \frac{1}{2\in}\boldsymbol{\xi}^{(k)}\left[f_0^{(k)}\left(\hat{\boldsymbol{y}}_+^{(k)}\right) - f_0^{(k)}\left(\hat{\boldsymbol{y}}_-^{(k)}\right)\right] + \frac{1}{2\in}\boldsymbol{\xi}^{(k)}\left(\lambda^{(k)}\right)^T\left[\boldsymbol{g}^{(k)}\left(\hat{\boldsymbol{y}}_+^{(k)}\right) - \boldsymbol{g}^{(k)}\left(\hat{\boldsymbol{y}}_-^{(k)}\right)\right] \tag{42}$$

where $\hat{\boldsymbol{y}}_+^{(k)}$ and $\hat{\boldsymbol{y}}_-^{(k)}$ are the measurement of $\hat{\boldsymbol{y}}^{(k)}$ with introduced perturbation $\pm \in \xi$.

With the Lagrangian approximated using (42), the model-free variant of (37) and (38) can be written as,

$$\boldsymbol{x}^{(k+1)} = \text{Proj}_{\boldsymbol{\chi}^{(k)}} \left\{ (1-\alpha)\boldsymbol{x}^{(k)} - \alpha \hat{\nabla} L^{(k)} \right\} \tag{43}$$

$$\boldsymbol{\lambda}^{(k+1)} = \text{Proj}\left\{ (1-\alpha)\boldsymbol{\lambda}^{(k)} + \alpha \boldsymbol{g}^{(k)}\left(\hat{\boldsymbol{y}}^{(k)}\right) \right\} \tag{44}$$

This model-free control algorithm quasi-linearly converges to the optimal solution; the proof can be found in [26] and will not be further elaborated.

3 Case study

3.1 Simulation setup

A modified IEEE 123-bus test feeder, as shown in Fig. 1, was adopted as the test distribution system in this study. The load data and line parameters can be found in [27]. It is assumed that seven DGs exist in the test system, including three diesel generators, two wind turbines, and two solar generation stations. The DG parameters are listed in Table 1. In addition, four tie lines—56-95, 83-95, 49-250, and 151-300—are added to the test system; thus, the modified system consists of 123 distribution nodes and 126 distribution lines.

The distribution system service restoration problem is solved during a 3-h horizon with a time resolution of 15 min. The forecasted wind and solar generation outputs are illustrated in Fig. 2. The real-time control algorithm will be solved every 2 s. The proposed distribution system service restoration model is solved by GAMS/CPLEX, and the real-time control algorithm is solved in MATLAB. To simulate the real-time fluctuations of renewable DGs, Gaussian noise will be added to each renewable DG as follows:

$$\hat{\boldsymbol{y}}_m^{(k)} = \boldsymbol{y}_m^{(k)} + W\boldsymbol{y}_m^{(k)} \tag{45}$$

where W denotes a random variable that follows a Gaussian distribution. The standard noise deviation was set to 0.1% for the simulation.

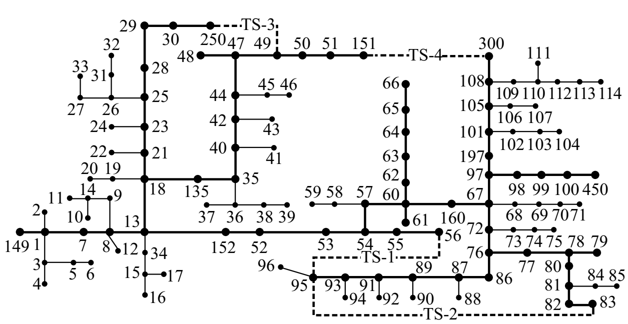

Fig. 1 Test system

Table 1 DG parameters

Bus no.	Type	Rating capacity/kVA	Power factor limit
21	Diesel	500	0.8
35	Solar	600	0.9
48	Wind	800	0.9
64	Diesel	500	0.8
78	Solar	600	0.9
95	Wind	800	0.9
105	Diesel	500	0.8

3.2 Simulation results

In this simulation, it is assumed that the upstream transmission system suffers from an outage, meaning that substation node 149 has no power supply. Assume that an outage occurs at 13:00. As shown in Fig. 2, both the solar generation and wind power outputs gradually decreased after 13:00. The distribution system reconfiguration is illustrated in Fig. 3, where switches 49-250, 50-51, 61-160, and 83-95 are open to maintain radiality. Table 2 lists the restoration results.

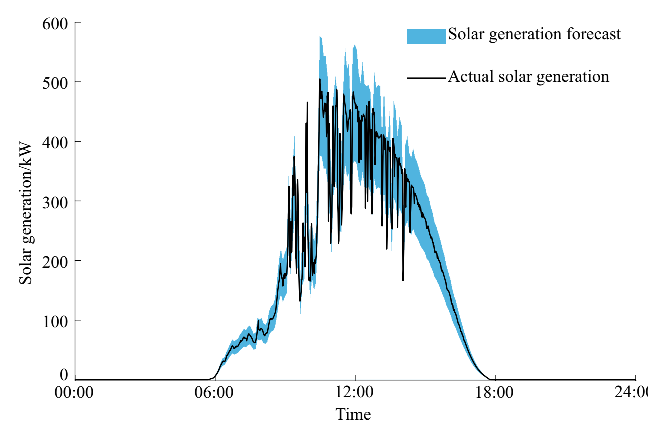

(a) Solar generation and forecast

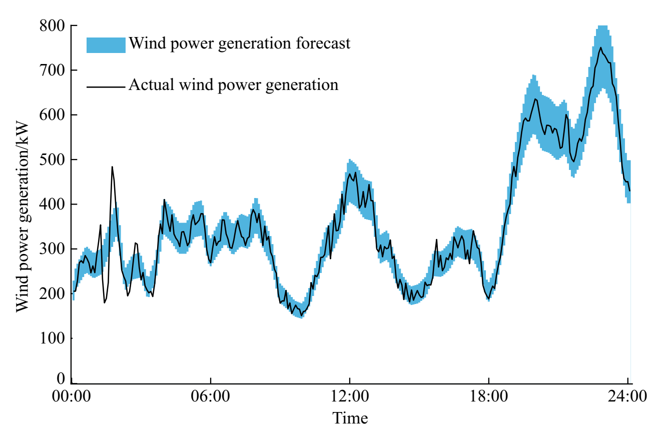

(b) Wind power generation and forecast

Fig. 2 Renewable DG generation and forecast profiles

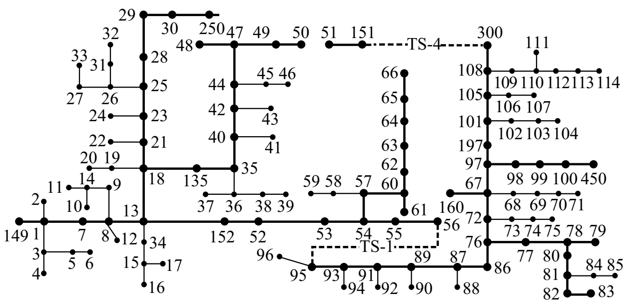

Fig. 3 Service restoration topology

As shown in Table 2, the available generation outputs of renewable DGs were efficiently used by the proposed restoration strategy. The optimization model proposed in Section 1 reconfigures the distribution system based on the conservative DG output forecast, and the real-time control algorithm is capable of tracking the trajectory of renewable DG output to avoid excessive renewable generation curtailment. The voltage magnitude was well controlled using the proposed strategy, and the power loss was minimized by reconfiguring the distribution system through switch operation.

Table 2 Performance of the developed restoration strategy

Item	Value
Average nodal voltage (p.u.)	0.988
Average network loss rate (%)	0.902
Total restored load consumption (kWh)	6736.9
Total renewable DG output (kWh)	3168.4
Actual available renewable DG output (kWh)	3218.3
Renewable DG utilization factor (%)	98.45

The performance of the real-time model-free control algorithm between 14:00 and 14:15 is illustrated in Figs. 4 and 5. Fig. 4 shows the total error between the scheduled renewable DG generation output and the actual DG generation capability. As shown in Fig. 4, the error is quite large at the beginning, when the real-time control algorithm first engaged. The large error is the result of the forecast error. By implementing the model-free control algorithm, the error rapidly decreases and fluctuates around zero. This fluctuation is caused by the real-time renewable DG generation fluctuation. It is validated that the real-time model-free control algorithm can effectively handle the forecast error and follow the random fluctuations of renewable DGs. In this way, the generation capacity of renewable DGs can be effectively used to restore the power supply in the distribution system after an outage.

Fig. 5 shows the generation profile of the wind power plant at node 48. In the beginning, the forecasted available generation output is near 235 kW in the restoration optimization model for the 14:00–14:15 period, whereas the actual wind power generation capacity is near 245 kW. Through the real-time control algorithm, the generation output of this wind power plant gradually increases to its maximum available output.

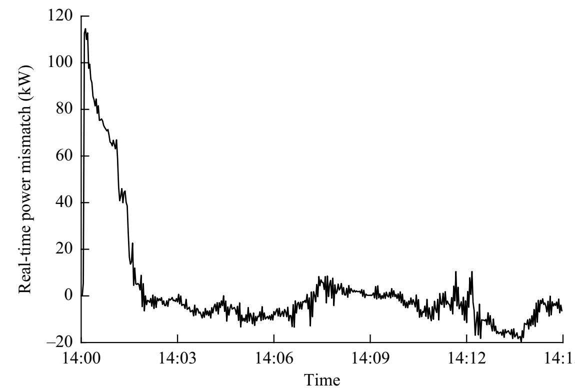

Fig. 4 Total real-time error between scheduled DG outputs and actual DG generation capability

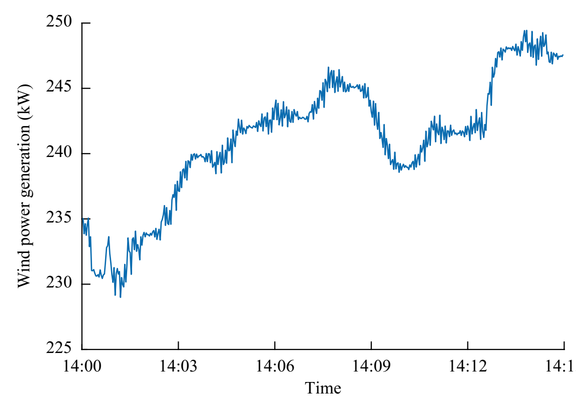

Fig. 5 Real-time wind power generation based on the model-free control algorithm

3.3 Comparative studies

In this subsection, the following methods are simulated to compare the performances of different distribution system restoration strategies:

M-1: Deterministic distribution system restoration method without real-time control [12];

M-2: Chance-constrained distribution system restoration model in Section 1.5 without real-time control;

M-3: The proposed integrated restoration and real-time control algorithm.

The total restored load consumption based on these three methods is compared in Table 3. As shown in Table 3, these methods were simulated in three scenarios. In the accurate forecast and no real-time variation scenario (2nd row in Table 3), method M-1 has the best performance because the chance constraints employed by M-2 and M-3 will introduce conservativeness in the renewable DG forecast. However, M-3 can restore more load compared to M-2 because the renewable DGs will modify their output in real time based on their capability, which can relieve the conservativeness of chance constraints to some extent. Meanwhile, method M-1 has the worst performance in the inaccurate forecast and no real-time variation scenario (3rd row in Table 3) because of the forecast error. When real-time variation is considered (4th row in Table 3), both M-1 and M-2 show considerable drops in restored load consumption compared to the 3rd row of Table 3. This is because the DG generation schedules cannot adapt to real-time capability, and real-time load shedding might be inevitable if renewable DG generation decreases. Conversely, the proposed method M-3 does a good job in tracking the trajectory of renewable DG real-time variations and the restored load consumption is almost identical to the scenario without real-time variation.

Therefore, it can be concluded from Table 3 that the deterministic method is only effective when accurate forecasts are available, which is generally not the case in practice. Without the real-time control algorithm, the chance-constrained optimization does not perform very well in terms of utilizing the available generation capacity because of the conservativeness of this method. The proposed method combines the chance-constrained approach and the real-time control algorithm to effectively handle the uncertainty of renewable DGs during the restoration stage.

Table 3 The restored load consumption in kWh

Scenario	M-1	M-2	M-3
Accurate forecast and no real-time variation	6864.5	6624.1	6741.1
Inaccurate forecast and no real-time variation	6581.0	6624.1	6741.1
Inaccurate forecast with real-time variation	6443.5	6494.7	6736.9

4 Conclusion

This study proposes a distribution system service restoration strategy using DGs as the primary power source to recover the load supply after an outage. The distribution system restoration problem is formulated as a mixed-integer SOCP model, where multiple DGs can be grouped into the same island. The uncertainty of renewable DGs is handled by a chance-constrained approach. Furthermore, the forecast error and real-time fluctuations of renewable DGs are managed by a model-free control algorithm. The control algorithm can track the trajectory of renewable generation without relying on information from accurate system models. Simulation results validated the proposed distribution system restoration strategy and demonstrated that the model-free control algorithm can successfully handle forecast errors and real-time fluctuations.

Intermittent renewable DGs should be accompanied by a variety of solutions to guarantee the success of distribution system restoration after outages and enhance the resilience of distribution systems. Possible options include mobile resource operation and connecting multiple distribution systems to networked microgrids. Further, local faults in distribution systems are not modeled in this study. If local faults exist, the islanding strategy and emergency cutoff planning for unexpected DG output decline should be considered in future work as well.

Acknowledgements

This work was authored by the National Renewable Energy Laboratory (NREL), operated by Alliance for Sustainable Energy, LLC, for the U.S. Department of Energy (DOE) under Contract No. DE-AC36-08GO28308. This work was supported by the U.S. Department of Energy Office of Electricity AOP Distribution Grid Resilience Project. The views expressed in the article do not necessarily represent the views of the DOE or the U.S. Government. The U.S. Government retains and the publisher, by accepting the article for publication, acknowledges that the U.S. Government retains a nonexclusive, paid-up, irrevocable, worldwide license to publish or reproduce the published form of this work, or allow others to do so, for U.S. Government purposes.

Declaration of Competing Interest

We declare that we have no conflicts of interest.

References

[1] Liu W, Sun L, Lin Z, et al (2016) Multi-objective restoration optimisation of power systems with battery energy storage systems. IET Gener Transm Distrib 10(7): 1749-1757

[2] Fthenakis V (2013) The resilience of PV during natural disasters: the hurricane Sandy case. In: Proceedings of the 2013 IEEE 39th Photovoltaic Specialists Conference, Tampa, FL, USA, 16-21 Jun 2013, 4p

[3] Qiu F, Li P (2017) An integrated approach for power system restoration planning. Proc. IEEE 105(7): 1234-1252

[4] Chen C, Wang J, Qiu F, et al (2016) Resilient distribution system by microgrids formation after natural disasters. IEEE Trans Smart Grid 7(2): 958-966

[5] Shirmohammadi D (1992) Service restoration in distribution networks via network reconfiguration. IEEE Trans Power Del 7(2): 952-958

[6] Mendes A, Boland N, Guiney P, et al (2013) Switch and tap-changer reconfiguration of distribution networks using evolutionary algorithms. IEEE Trans Power Syst 28(1): 85-92

[7] Chen WH (2010) Quantitative decision-making model for distribution system restoration. IEEE Trans Power Syst 25(1): 313-321

[8] Lim SI, LEE SJ, Choi SM, et al (2006) Service restoration methodology for multiple fault case in distribution systems. IEEE Trans Power Syst 21(4): 1638-1644

[9] Miu KN, Chiang HD, McNulty RJ (2000) Multi-tier service restoration through network reconfiguration and capacitor control for large-scale radial distribution networks. IEEE Trans Power Syst 15(3): 1001-1007

[10] Nguyen CP, Flueck AJ (2012) Agent based restoration with distributed energy storage support in smart grids. IEEE Trans. Smart Grid 3(2): 1029-1038

[11] Kumar V, Kumar RHC, Gupta I, et al (2010) DG integrated approach for service restoration under cold load pickup. IEEE Trans Power Del 25(1): 398-406

[12] Liu W, Ding F, Zhao C (2020) Dynamic restoration strategy for distribution system resilience enhancement. In: Proceedings of the 2020 IEEE Power & Energy Society Innovative Smart Grid Technologies Conference, Washington, DC, USA, 17-20 Feb 2020, 5p

[13] Moreira CL, Resende FO, Lopes JAP (2007) Using low voltage microgrids for service restoration. IEEE Trans. Power Syst 22(1): 395-403

[14] Wang Z, Wang J (2017) Service restoration based on AMI and net-worked MGs under extreme weather events. IET Gener Transm Distrib 11(2): 401-408

[15] Li J, Ma XY, Liu CC, et al (2014) Distribution system restoration with microgrids using spanning tree search. IEEE Trans Power Syst 29(6): 3021-3029

[16] Chen X, Wu W, Zhang B (2016) Robust restoration method for active distribution networks. IEEE Trans Power Syst 31(5): 4005-4015

[17] Bernstein A, Dall'Anese E, Simonetto A (2019) Optimal power flow pursuit. IEEE Trans Smart Grid 9(2): 942-952

[18] Hauswirth A, Subotic I, Bolognani S, et al (2018) Time-varying projected dynamical systems with applications to feedback optimization of power systems. In: Proceedings of the 2018 IEEE Conference on Decision and Control, Miami Beach, FL, USA, 17-19 Dec 2018, 3258-3263

[19] Taylor JA, Hover FS (2012) Convex models of distribution system reconfiguration. IEEE Trans Power Syst 27(3): 1407-1413

[20] Capitanescu F, Bilibin I, Ramos ER (2014) A comprehensive centralized approach for voltage constraints management in active distribution grid. IEEE Trans Power Syst 29(2): 933-942

[21] Gan L, Li N, Topcu U, et al (2013) Optimal power flow in tree networks. In: Proceedings of the 2013 52nd IEEE Conference on Decision and Control, Florence, Italy, 10-13 Dec 2013, 6p

[22] Malekpour AR, Pahwa A, Das S (2013) Inverter-based var control in low voltage distribution systems with rooftop solar PV. In: Proceedings of the 45th North America Power Symposium, Manhattan, KS, USA, 22-24 Sep 2013, 5p

[23] Shu Z, Jirutitijaroen P (2011) Latin hypercube sampling techniques for power system reliability analysis with renewable energy sources. IEEE Trans Power Syst 26(4): 2066-2073

[24] Roald F, Andersson G (2018) Chance-constrained AC optimal power flow: reformulations and efficient algorithms. IEEE Trans Power Syst 33(3): 2906-2918

[25] Liu W, Zhan J, Chung CY, et al (2019) Day-ahead optimal operation for multi-energy residential systems with renewables. IEEE Trans Sustain Energy 10(4): 1927-1938

[26] Chen Y, Bernstein A, Devraj A, et al (2020) Model-free primal-dual methods for network optimization with application to real-time optimal power flow. In: Proceedings of the 2020 American Control Conference, Denver, CO, USA, 1-3 Jul 2020, 8p

[27] IEEE PES AMPS DSAS Test Feeder Working Group (2020). PES test feeders. https://site.ieee.org/pes-testfeeders/resources/. Accessed 10 Dec 2020

Biographies

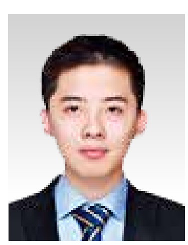

Weijia Liu received the B. Eng. and Ph.D. degrees in electrical engineering from Zhejiang University, Hangzhou, China, in 2011 and 2016, respectively. He is currently a researcher at the Power Systems Engineering Center, National Renewable Energy Laboratory, Golden, CO, USA. His research interests include power system restoration and resilience, integrated energy systems, and smart grid.

Yue Chen received the Ph.D. degree in electrical and computer engineering from the University of Florida in 2016. He is currently a researcher at the Power Systems Engineering Center, National Renewable Energy Laboratory, Golden, CO, USA. His research focuses on data-driven control and optimization techniques with power system applications.

Fei Ding received the B.S. and M.S. degrees from Tianjin University, China, in 2008 and 2010, respectively and the Ph.D. degree from Case Western Reserve University in 2014. She is currently a senior research engineer at the National Renewable Energy Laboratory (NREL), Golden, CO, USA. Her research interests include renewable energy grid integration, distributed energy resource aggregation and controls, and grid resilience and security. She is leading multiple projects at NREL on developing advanced models and controls for managing grid-edge resources to enhance grid flexibility, reliability, and resilience, and to develop a new advanced distribution management system and distributed energy resource management system applications to modernize emerging distribution grids. She has secured multimillion-dollar funding for NREL to advance distribution grid operations and resilience.

(Editor Yanbo Wang)